IJICTR
International Journal of Information & Communication Technology Research

Volume 13- Number 2 – 2021 (29 -38)

PolSAR Classification Using Contextual Based Locality Preserving Projection and Guided Filtering

Maryam Imani*
Faculty of Electrical and Computer Engineering
Tarbiat Modares University
Tehran, Iran
maryam.imani@modares.ac.ir

Received: 4 April 2021 - Accepted: 23 May 2021

Abstract—**Contextual feature extraction is studied for polarimetric synthetic aperture radar (PolSAR) image classification in this work. The contextual locality preserving projection (CLPP) method is proposed for generation of contextual feature cubes using limited training samples. The local information in neighborhood regions is used to extend the training set by including the spatial information. Then, a supervised transform is applied to the polarimetric-contextual feature cube to reduce the data dimensionality while preserves the local structures and settles the samples belonging to the same class close together. Finally, a guided filter is applied to the classification map to degrade the speckle noise. The classification results on two real L-band PolSAR data from AIRSAR show superior performance of CLPP for PolSAR classification in small sample size situations.**

Keywords—***locality preserving projection; spatial feature extraction; classification; polarization; classification; guided filter.***

I. INTRODUCTION

One of the main challenges in polarimetric synthetic aperture radar (PolSAR) classification is extraction of features with high discrimination ability [1]. A high resolution SAR image contains rich contextual information, which can be very effective to provide an accurate classification map from the ground surface [2]. From the other hand, a PolSAR data is the SAR image from the same scene acquired in multiple polarizations. Different polarimetric characterizations of different materials allow class discrimination among various classes.

In recent years, deep learning attracts much attention from the researchers of various fields such as remote sensing [3]. For SAR and PolSAR classification, many deep learning based methods have been proposed. In [4], a sparse filtering and manifold regularization based deep neural network is introduced for feature extraction and classification of PolSAR image. A three channel convolutional neural network, which utilizes the ability of unlabeled samples to improve the PolSAR image classification, is proposed in [5]. It not only utilizes a spatial weighted method for increasing the role of central pixel but also includes deep and scale polarization information to the

* Corresponding Author

[DOI: 10.52547/itrc.13.2.29]

classification process. Generally, although deep learning based methods have shown great performance in the feature extraction and classification of SAR and PolSAR images, but, they require a sufficiently large training set to have a reasonable performance.

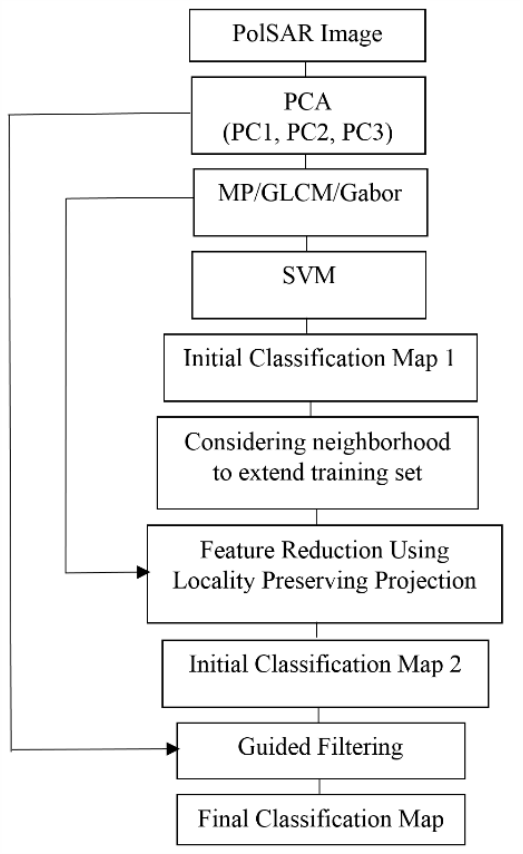

Fig. 1. Block Diagram of CLPP with guided filtering

To explain the scattering process of different class types in a PolSAR image, a decision tree based approach is introduced in [6] where the polarimetric features are utilized at the tree nodes. A multi-view deep forest is also suggested in [7] by involving online learning. To deal with imbalanced sample size in various classes, a cost sensitive latent space learning is suggested in [8], which reduces the learning bias.

The use of textural features extractors can be very useful for classification of high resolution images with rich spatial details. Among various contextual operators, gray level co-occurrence matrix (GLCM) is well known [9]. It measures that how much probability, two different gray levels occur in the neighboring of a given pixel. The Gabor filter banks have also shown great success in textural feature extraction in multiple scales and directions [10]. The morphological operators analyze how much the image interacts with a set of structure elements with various shapes and sizes [11]-[12]. The output results of opening and closing morphological operators by reconstruction are concatenated together to provide a morphological profile (MP).

The PolSAR image classification is a challenging task due to limited number of training samples and also contamination of SAR images to the speckle noise. In addition, spatial information of the PolSAR image should appropriately be extracted and fused with the polarimetric features. To deal with these difficulties of the PolSAR image classification, the contextual based locality preserving projection (CLPP) is proposed in this work. According to CLPP, the ability of unlabeled samples is utilized through implementing an initial classification by using polarimetric information and contextual features extracted by morphological filters, GLCM operators and Gabor filter bank. Then, the neighborhood information in the obtained classification map is used to extend the training set. After that, concatenation of the PolSAR cube with the extracted feature maps beside the enlarged training set are used to find a new classification map. The support vector machine (SVM) is used as classifier in this work because it has shown great efficiency in small sample size situations [13]. Finally, the guided filter is applied to the classification map to reduce the speckle noise and improve the classification accuracy.

The classification results on two real PolSAR data show efficiency of CLPP in improvement of the classification performance with respect to the conventional MP, GLCM and Gabor feature cubes.

II. Proposed Method

A) *PolSAR representation*

Each pixel of the PolSAR image is represented by its coherency matrix:

$$\boldsymbol{T} = \begin{bmatrix} T_{11} & T_{12} & T_{13} \\ T_{12}^{*} & T_{22} & T_{23} \\ T_{13}^{*} & T_{23}^{*} & T_{33} \end{bmatrix} \quad (1)$$

where $(\cdot)^{*}$ denotes the conjugate operator. A PolSAR image can be represented with a cube containing 9 polarimetric channels where each channel is the real or imaginary value of each element of the coherency matrix [14] as follows:

$$\boldsymbol{f} = [T_{11}, T_{22}, T_{33}, Re(T_{12}), Im(T_{12}), Re(T_{13}), Im(T_{13}), Re(T_{23}), Im(T_{23})] \quad (2)$$

where $Re(\cdot)/Im(\cdot)$ is the real/imaginary part of $(\cdot)$ and $T_{ij}; i, j = 1,2,3$ are the elements of the coherency matrix $\boldsymbol{T}$ in (1).

The block diagram of the proposed CLPP method is shown in Fig. 1. The proposed CLPP method, at first, produces a spatial feature cube from the PolSAR image. The extracted feature cube has high dimensionality and needs to feature reduction. For

[DOI: 10.52547/itrc.13.2.29]

dimensionality reduction, a feature projection with involving the class labels information is preferred. To this end, enough training samples are required to well model the polarimetric-contextual structure of the PolSAR data in various classes. The CLPP method is implemented according to the following steps:

1- The contextual features are extracted from the PolSAR image by applying morphological filters, GLCM operators and Gabor filter banks.
2- The contextual feature cube (MP, GLCM or Gabor) is given to the SVM classifier to find an initial classification map.
3- The neighborhood information in the initial classification map is used to provide a new set of training samples from the original unlabeled samples. The result is extension of training set.
4- A supervised locality preserving projection is used for dimensionality reduction of the contextual feature cube obtained from the first step. It involves the class label information of the enlarged training set obtained from step 3.
5- The features extracted from step 4 and the enlarged training set obtained from step 3 are given to the SVM classifier to results in a new classification map.
6- Guided filtering is applied to the classification map obtained in step 5 to reduce the speckle noise.

The steps 1, 3, 4 and 6 from the above classification process are explained with more details in the following.

B) Extraction of spatial feature cube

Because, the PolSAR data is a polarimetric feature cube, the principal component analysis is applied to the PolSAR data. Some principal components (PCs) of PolSAR image are chosen and the contextual operators are applied to each PC. For example, to provide the GLCM feature cube, the GLCM operator is applied to each PC of PolSAR. Then, the GLCM feature maps obtained from all PCs are concatenated to the original PolSAR cube to results in the GLCM feature cube. The MP and Gabor feature cubes are obtained in a similar way.

MP: The common opening and closing morphological operators are constructed by the basic morphological operators, i.e., erosion and dilation. The reconstruction filters do not produce discontinuities and preserve the shapes observed in given images. With Applying n opening operators by reconstruction (with n different sizes of structure elements), and n closing ones, $2n$ output images containing shape and contextual information are resulted.

$$MP_n(I) = \{\varphi_1(I), \dots, \varphi_n(I), I, \gamma_1(I), \dots, \gamma_n(I)\} \quad (3)$$

where $\varphi_i(I)$ and $\gamma_i(I)$; $i = 1,2, \dots, n$ are closing and opening filters by reconstruction, respectively.

GLCM: GLCM is a square matrix that reveals some properties about spatial distribution of gray levels of the input image with considering relationship among the neighboring pixels. For each centered pixel, the number of pixels with a considered grey level in the specific distance and direction is accounted. This process is done for all possible gray levels. Corresponding to each pixel, a GLCM matrix is composed. Then, spatial features such as contrast, correlation, variance, entropy and some other ones are extracted from the GLCM matrix [19].

Gabor: A Gabor filter bank provides the localization characteristics in both spatial and frequency domains in various scales and directions. A Gabor filter is a sinusoidal wave multiplied by a Gaussian function, which is convolved with the input image to generate the Gabor features.

C) Neighborhood information

The initial classification map is obtained by the contextual feature cube containing both polarimetric and spatial features. The efficient SVM classifier with low sensitivity to the number of training samples is used to obtain the classification map. So, the initial labels assigned to the pixels are relatively high reliable. Let consider a local window with the length of $L \times L$ around the central pixel $\boldsymbol{x}_i$ in the initial classification map. The neighborhood pixels can be represented as:

$$N(\boldsymbol{x}_i) = \{\boldsymbol{x}_i^n \triangleq (p,q); p \in [p_i - a, p_i + a], q \in [q_i - a, q_i + a]\} \quad (4)$$

where (p_i, q_i) is the pixel coordinate of ith training sample, $a = (L-1)/2$, $\boldsymbol{x}_i^n$; $n = 1,2, \dots, K$ is n th spatial neighbor of $\boldsymbol{x}_i$, and $K = L^2 - 1$ denotes the number of neighbors. Among the neighboring pixels, those that have the same label as the central pixel are added to the training samples to enlarge the training set. So:

$$\text{if } l_{\boldsymbol{x}_i^n} = l_{\boldsymbol{x}_i}, \text{ then } \boldsymbol{x}_i^n \text{ is added to the training set}$$

Adding the spatial neighbors to the training set has two main advantages [15]: 1- involving spatial information to the classification process and 2- enlarging the training set to deal with small sample size situations.

D) Supervised feature space projection

Inspired from [15], the enlarged training set is used for dimensionality reduction through a feature space transform with preserving the local structure of data. An adjacency graph is constructed by using the training samples in the polarimetric-contextual feature space. Let denote $\mathbf{Z}=[\boldsymbol{z}_1, \boldsymbol{z}_2, \dots, \boldsymbol{z}_N]$ as the enlarged training set where N is the number of samples in the extended training set. A projection matrix $\mathbf{A}$ is sought which transforms the sample $\boldsymbol{z}_i$ $(i = 1,2, \dots, N)$ to $\boldsymbol{y}_i =$

[DOI: 10.52547/itrc.13.2.29]

$\mathbf{Az}_i$ such that not only preserves the locality of data but also leads to close the samples with the same class labels in the projected feature space. In order to compute the projection matrix $\mathbf{A}$, the following optimization problem is solved:

$$\mathbf{A} = arg\min_{\mathbf{A}} \sum_{i=1}^{N}\sum_{j=1}^{N} \|\boldsymbol{y}_i - \boldsymbol{y}_j\|^2 w_{ij} \quad (5)$$

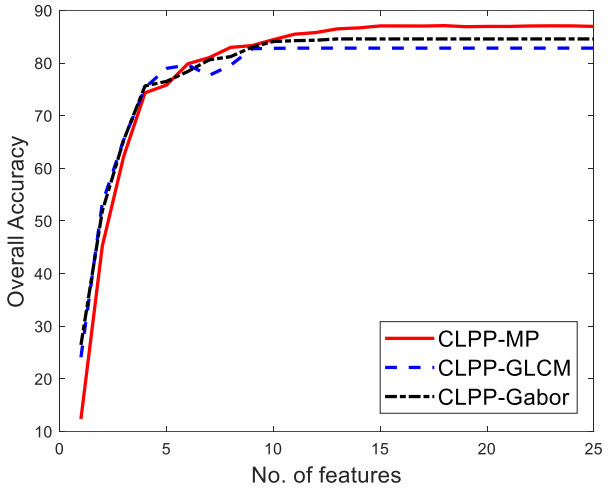

Fig. 2. OA versus the number of extracted features for Flevoland dataset. The results are obtained by the first PC and $L = 7$.

that with replacing $\boldsymbol{y}_i = \mathbf{Az}_i$, we have:

$$\mathbf{A} = arg\min_{\mathbf{A}} \sum_{i=1}^{N}\sum_{j=1}^{N} \|\mathbf{A}^T\boldsymbol{z}_i - \mathbf{A}^T\boldsymbol{z}_j\|^2 w_{ij}$$
$$= arg\min_{\mathbf{A}} \mathrm{tr}(\mathbf{A}^T\mathbf{ZLZ}^T\mathbf{A}) \quad (6)$$

$\mathbf{L} = \mathbf{D} - \mathbf{W}$ is the Laplacian matrix where $\mathbf{D}$ denotes a diagonal matrix of the column sums of $\mathbf{W}$ and $\mathbf{W}$ indicates the similarity matrix defined by $w_{ij} = 1$ (if $l_{x_i} = l_{x_j}$) and $w_{ij} = 0$ $\left(\text{if } l_{x_i} \neq l_{x_j}\right)$; $i, j = 1,2,\dots,N$ where l_{x_i} is the class label of sample $\boldsymbol{x}_i$. The eigenvectors associated with the smallest eigenvalues of the matrix $\mathbf{ZLZ}^T$ compose the projection matrix $\mathbf{A}$.

E) Guided Filtering

After feature extraction in step 4, the extracted features are fed to the SVM to provide a new classification map (initial classification map 2). Due to high value of speckle noise in SAR images, the guided filter is suggested to degrade the speckle noise and smooth the classification map. In a PolSAR image with M pixels and n_c classes, n_c binary probability maps $\{Prob_1, Prob_2, \dots, Prob_{n_c}\}$ are considered corresponding to the initial classification map 2 where $Prob_i \in \mathcal{R}^{r\times c}$ is ith binary probability map, and r/c is the number of rows/columns. The binary probability map is obtained by [16]-[17]:

$$Prob_{i,j} = \begin{cases} 1; & \boldsymbol{x}_j \in class\ i \\ 0; & \boldsymbol{x}_j \in class\ k; k \neq i \end{cases}$$
$$i = 1, \dots, n_c; j = 1, \dots, M \quad (7)$$

In other words, $Prob_{i,j} = 1$ if pixel j belongs to class i and otherwise, $Prob_{i,j} = 0$. The probability maps are filtered by:

$$\widehat{Prob}_{i,j} = \sum_j W_{i,j}(G)\, Prob_{i,j} \quad (8)$$

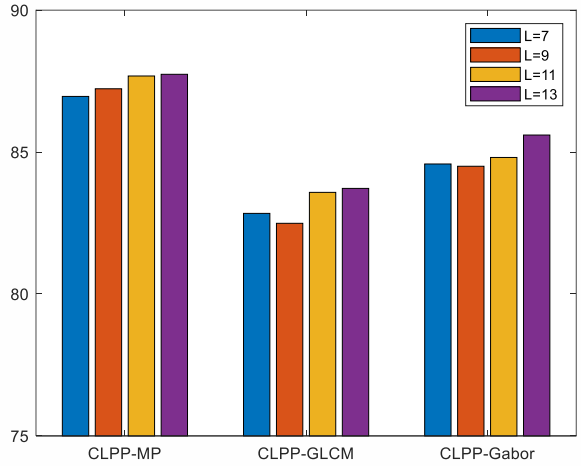

Fig. 3. OA for different window lengths in Flevoland dataset. The results are obtained by the first PC and 20 extracted features.

where i /j indicate the indix of the pixel i/j; G is the guidance image and $W_{i,j}(G)$ denotes the filtering weight computed by:

$$W_{i,j}(G) = \frac{1}{|w|^2}\sum_{k\in w_i, k\in w_j}\left(1 + \frac{(G_i-\mu_k)(G_j-\mu_k)}{\sigma_k^2+\varepsilon}\right) \quad (9)$$

w_i represents the local window around the pixel i; μ_k/σ_k is the mean/standard deviation of G in w_k, and $|w|$ is the number of pixels in window w_k. The filter preserves the edges according to the guidance image G. The first principal component of the PolSAR data is considered as G. The use of $\widehat{Prob}_{i,j};\ i = 1, \dots, n_c; j = 1, \dots, M$ not only utilizes more contextual information in the classification process but also leads the probability maps to align with the real class boundaries. After guided filtering, the label of pixel j is obtained by applying the maximum decision rule as follows:

$$l_j = \arg\max_{i=1,\dots,n_c} Prob_{i,j};\ j = 1, \dots, M \quad (10)$$

III. Experiments

A) Datasets and parameter settings

To assess the classification performance of CLPP, two real L-band PolSAR images acquired by AIRSAR are utilized to implement experiments. The used datasets are Flevoland, an 900×1024 image with 15 classes; and SanFrancisco, an 750×1024 image with 4 classes. To evaluate the sample size situation, only 10 training samples per class are used in both datasets.

[DOI: 10.52547/itrc.13.2.29]

TABLE I. CLASSIFICATION RESULTS OF CLPP (WITHOUT GUIDED FILTERING) COMPARED TO FULL BAND CONTEXTUAL CUBES FOR FLEVOLAND DATASET. THE RESULTS ARE OBTAINED BY THREE PCS, $L = 7$ AND 18 EXTRACTED FEATURES.

No	Name of class	# Total Samples	CLPP-MP	CLPP-GLCM	CLPP-Gabor	MP	GLCM	Gabor
1	Stembeans	6103	94.87	87.12	91.33	96.00	81.48	82.93
2	Peas	9111	97.60	93.40	92.53	96.85	92.31	91.47
3	Forest	14944	90.06	83.32	83.20	90.50	77.08	67.92
4	Lucerne	9477	92.11	87.19	86.08	91.76	86.35	87.35
5	Wheat	17283	97.96	79.34	78.30	90.99	80.65	79.27
6	Beet	10050	85.71	87.37	93.07	92.00	89.94	91.13
7	Potatoes	15292	94.96	90.68	93.92	95.47	91.97	87.52
8	Bare soil	3078	100.00	99.94	99.94	100.00	99.97	99.84
9	Grass	6269	99.84	76.68	91.26	99.25	66.95	74.21
10	Rapeseed	12690	94.94	84.09	78.87	96.10	74.14	75.34
11	Barely	7156	96.41	94.42	96.24	96.48	95.96	96.60
12	Wheat 2	10591	83.51	76.38	80.03	70.14	73.02	69.31
13	Wheat 3	21300	95.28	78.48	88.21	97.69	69.55	80.30
14	Water	13476	97.20	78.87	79.02	83.36	63.61	62.32
15	Buildings	476	96.22	77.73	76.68	94.33	78.57	77.94
Average Accuracy			**94.45**	**85.00**	**87.25**	**92.73**	**81.44**	**81.56**
Overall Accuracy			**94.04**	**83.93**	**86.35**	**92.05**	**79.58**	**79.77**
Kappa			**93.50**	**82.52**	**85.14**	**91.34**	**77.83**	**78.02**

TABLE II. Z SCORES OBTAINED BY THE MCNEMARS TEST FOR FLEVOLAND DATASET (CLPP WITHOUT GUIDED FILTERING).

	CLPP-MP	CLPP-GLCM	CLPP-Gabor	MP	GLCM	Gabor
CLPP-MP	0	104.10	88.23	34.98	131.29	130.38
CLPP-GLCM	-104.10	0	-34.73	-89.91	53.51	47.49
CLPP-Gabor	-88.23	34.73	0	-70.95	73.71	73.59
MP	-34.98	89.91	70.95	0	120.67	120.40
GLCM	-131.29	-53.51	-73.71	-120.67	0	-3.04
Gabor	-130.38	-47.49	-73.59	-120.40	3.04	0

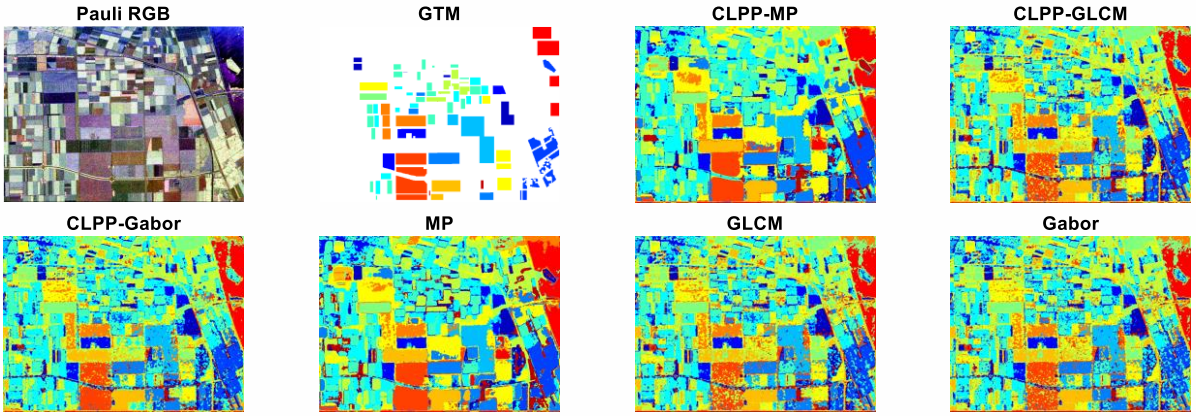

Figure 4. RPL Comparison of classification maps obtained by CLPP (without guided filtering) and contextual feature cubes for Flevoland dataset.

[DOI: 10.52547/itrc.13.2.29]

TABLE III. CLASSIFICATION RESULTS OF CLPP (WITHOUT GUIDED FILTERING) COMPARED TO FULL BAND CONTEXTUAL CUBES FOR SANFRANCISCO DATASET. THE RESULTS ARE OBTAINED BY THREE PCS, $L = 7$ AND 18 EXTRACTED FEATURES.

No	Name of class	# Total Samples	CLPP-MP	CLPP-GLCM	CLPP-Gabor	MP	GLCM	Gabor
1	Mountain	61913	82.56	83.94	83.33	80.35	86.56	78.68
2	Grass	135282	72.91	73.02	78.39	67.18	76.04	80.84
3	Sea	348639	92.40	87.62	87.20	88.40	82.57	95.68
4	Building	375766	77.57	66.48	64.24	81.10	65.37	64.34
Average Accuracy			**81.36**	**77.77**	**78.29**	**79.26**	**77.63**	**79.89**
Overall Accuracy			**82.83**	**76.61**	**76.29**	**81.77**	**74.87**	**79.58**
Kappa			**75.10**	**67.02**	**66.71**	**73.68**	**65.02**	**70.89**

TABLE IV. Z SCORES OBTAINED BY THE MCNEMARS TEST FOR SANFRANCISCO DATASET (CLPP WITHOUT GUIDED FILTERING).

	CLPP-MP	CLPP-GLCM	CLPP-Gabor	MP	GLCM	Gabor
CLPP-MP	0	139.95	146.18	33.20	170.05	78.29
CLPP-GLCM	-139.95	0	10.92	-109.12	45.24	-75.19
CLPP-Gabor	-146.18	-10.92	0	-115.12	36.61	-87.31
MP	-33.20	109.12	115.12	0	138.68	48.93
GLCM	-170.05	-45.24	-36.61	-138.68	0	-158.83
Gabor	-78.29	75.19	87.31	-48.93	158.83	0

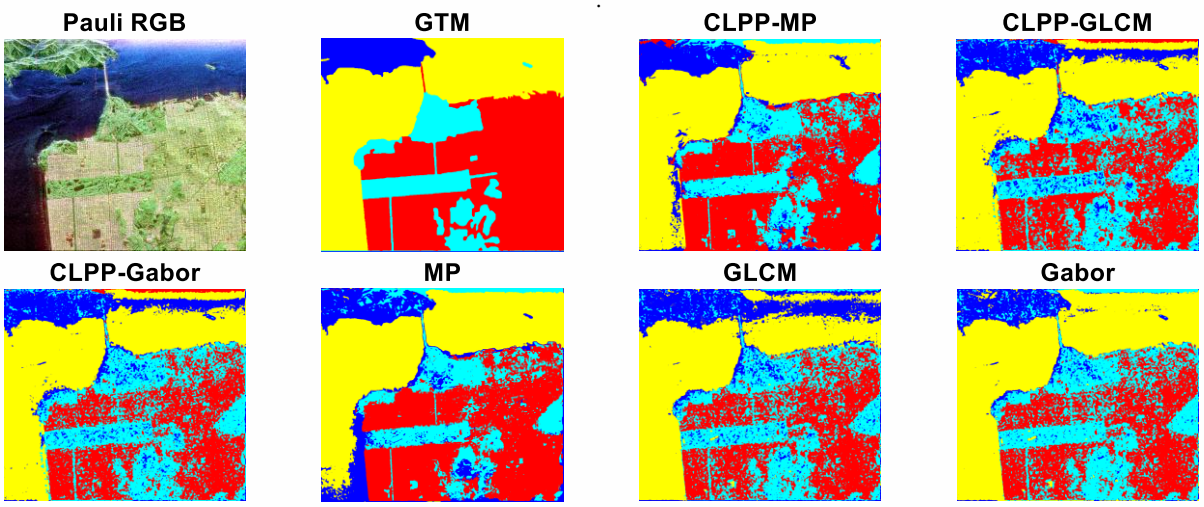

Figure 5. Comparison of classification maps obtained by CLPP (without guided filtering) and contextual feature cubes for SanFrancisco dataset.

TABLE V. CLASSIFICATION RESULTS OF CLPP (WITH GUIDED FILTERING) COMPARED TO FULL BAND CONTEXTUAL CUBES FOR FLEVOLAND DATASET. THE RESULTS ARE OBTAINED BY THREE PCS, $L = 7$ AND 18 EXTRACTED FEATURES.

No	Name of class	# Total Samples	CLPP-MP	CLPP-GLCM	CLPP-Gabor	MP	GLCM	Gabor
1	Stembeans	6103	97.62	97.67	97.08	96.59	96.23	97.33
2	Peas	9111	99.86	99.42	99.20	99.91	99.23	98.96
3	Forest	14944	90.60	96.69	90.50	90.60	91.37	90.24
4	Lucerne	9477	92.10	94.56	93.63	93.09	92.05	94.15
5	Wheat	17283	99.37	88.08	91.41	96.45	91.66	91.78
6	Beet	10050	87.86	97.84	98.68	93.97	97.16	97.95
7	Potatoes	15292	98.87	99.61	99.12	98.97	99.41	99.23
8	Bare soil	3078	100.00	100.00	100.00	100.00	100.00	100.00
9	Grass	6269	100.00	99.54	100.00	100.00	99.94	100.00
10	Rapeseed	12690	99.52	97.71	95.40	99.87	91.28	92.30
11	Barely	7156	99.43	99.89	99.96	99.30	100.00	100.00
12	Wheat 2	10591	86.39	88.89	98.70	65.87	93.36	88.24
13	Wheat 3	21300	97.65	99.54	99.95	99.51	91.77	99.88
14	Water	13476	98.18	83.12	83.47	82.96	66.17	64.38
15	Buildings	476	93.70	83.19	83.19	97.27	83.19	83.19
Average Accuracy			**96.08**	**95.05**	**95.35**	**94.29**	**92.86**	**93.18**
Overall Accuracy			**96.10**	**95.23**	**95.50**	**93.80**	**92.14**	**92.92**
Kappa			**95.75**	**94.80**	**95.10**	**93.24**	**91.45**	**92.28**

[DOI: 10.52547/itrc.13.2.29]

TABLE VI. Z SCORES OBTAINED BY THE MCNEMARS TEST FOR FLEVOLAND DATASET (CLPP WITH GUIDED FILTERING).

	CLPP-MP	CLPP-GLCM	CLPP-Gabor	MP	GLCM	Gabor
CLPP-MP	0	14.95	10.83	45.37	57.79	48.66
CLPP-GLCM	-14.95	0	-7.39	27.66	55.28	46.08
CLPP-Gabor	-10.83	7.39	0	32.09	68.51	59.13
MP	-45.37	-27.66	-32.09	0	25.94	15.25
GLCM	-57.79	-55.28	-68.51	-25.94	0	-21.18
Gabor	-48.66	-46.08	-59.13	-15.25	21.18	0

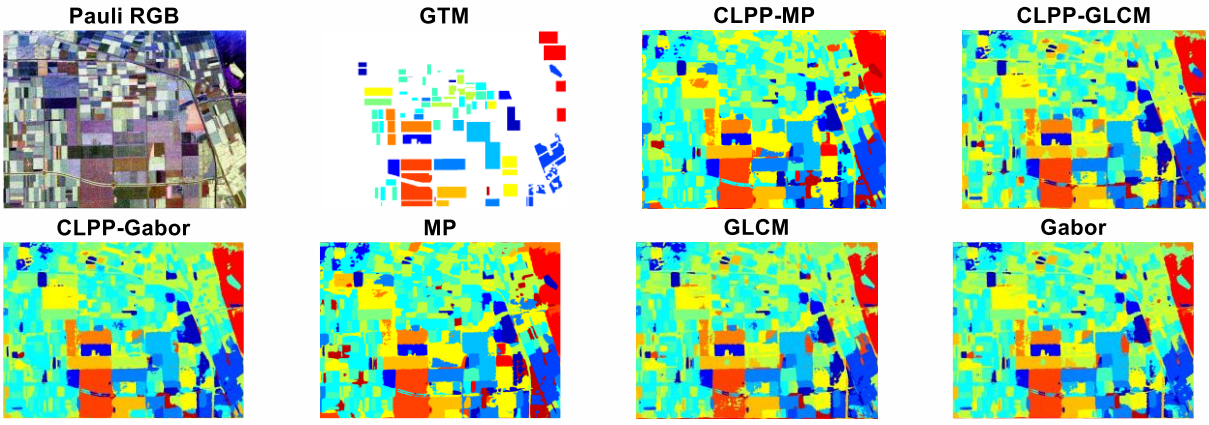

Figure 6. Comparison of classification maps obtained by CLPP (with guided filtering) and contextual feature cubes for Flevoland dataset

TABLE VII. CLASSIFICATION RESULTS OF CLPP (WITH GUIDED FILTERING) COMPARED TO FULL BAND CONTEXTUAL CUBES FOR SANFRANCISCO DATASET. THE RESULTS ARE OBTAINED BY THREE PCS, $L = 7$ AND 18 EXTRACTED FEATURES.

No	Name of class	# Total Samples	CLPP-MP	CLPP-GLCM	CLPP-Gabor	MP	GLCM	Gabor
1	Mountain	61913	89.38	93.45	93.29	86.39	94.69	89.30
2	Grass	135282	72.32	86.68	90.27	67.41	88.42	89.26
3	Sea	348639	97.05	92.22	92.07	90.44	81.87	98.01
4	Building	375766	86.80	79.08	72.52	90.74	76.74	73.44
Average Accuracy			**86.39**	**87.86**	**87.04**	**83.74**	**85.43**	**87.50**
Overall Accuracy			**88.73**	**86.13**	**83.91**	**86.91**	**81.60**	**86.12**
Kappa			**83.13**	**79.83**	**76.92**	**80.48**	**73.89**	**79.82**

TABLE VIII. Z SCORES OBTAINED BY THE MCNEMARS TEST FOR SANFRANCISCO DATASET (CLPP WITH GUIDED FILTERING).

	CLPP-MP	CLPP-GLCM	CLPP-Gabor	MP	GLCM	Gabor
CLPP-MP	0	86.04	133.37	73.35	183.98	84.90
CLPP-GLCM	-86.04	0	103.38	-20.28	154.64	0.22
CLPP-Gabor	-133.37	-103.38	0	-69.15	84.45	-91.10
MP	-73.35	20.28	69.15	0	117.19	20.44
GLCM	-183.98	-154.64	-84.45	-117.19	0	-145.58
Gabor	-84.90	-0.22	91.10	-20.44	145.58	0

[DOI: 10.52547/itrc.13.2.29]

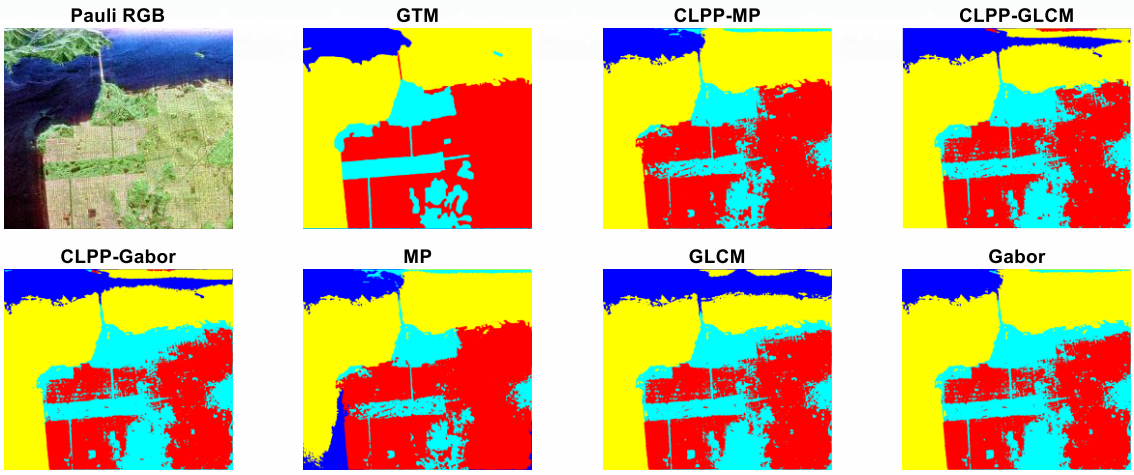

Figure 7. Comparison of classification maps obtained by CLPP (with guided filtering) and contextual feature cubes for SanFrancisco dataset.

TABLE IX. COMPARISON OF OVERALL ACCURACY AMONG METHODS WITHOUT GUIDED FILTERING AND WITH GUIDED FILTERING.

Dataset	Filtering	CLPP-MP	CLPP-GLCM	CLPP-Gabor	MP	GLCM	Gabor
Flevoland	Without guided filtering	94.04	83.93	86.35	92.05	79.58	79.77
	With guided filtering	96.10	95.23	95.50	93.80	92.14	92.92
SanFrancisco	Without guided filtering	82.83	76.61	76.29	81.77	74.87	79.58
	With guided filtering	88.73	86.13	83.91	86.91	81.60	86.12

TABLE X. RUNNING TIME OF DIFFERENT METHODS (SECONDS).

Dataset	CLPP-MP	CLPP-GLCM	CLPP-Gabor	MP	GLCM	Gabor
Flevoland	73.88	193.09	69.66	57.63	179.63	56.26
SanFrancisco	50.21	218.43	60.59	44.23	214.20	56.33

The first PC or some first PCs of the PolSAR images can be used to compose the contextual feature cubes (MP, GLCM and Gabor). The MP composed from each PC contains 73 channels obtained by applying 36 opening filter and 36 closing filters by reconstruction. To build the GLCM matrix from each PC, the fast GLCM algorithm with distance $d = 1$ and direction $\theta = 0$ with a 7×7 neighborhood window is just, the first PC of the PolSAR data is used to compute the contextual cubes (MP, GLCM and Gabor). Fig. 2 shows the overall accuracy (OA) versus the number of extracted features in the fourth step of the CLPP method for Flevoland dataset. $L = 7$ is fixed as the neighborhood window length. As seen, with increasing the number of extracted features, the OA is increased to a dimensionality and after that, it becomes stable. Another finding is that the best results are achieved by CLPP-MP where CLPP-MP means that CLPP is implemented with the MP contextual feature cube obtained in the first step. After CLPP-MP, CLPP-Gabor and then, CLPP-GLCM are preferred in the Flevoland dataset. In another experiment, influence of the length of neighborhood window $L \times L$ used in the third step of the CLPP method is assessed. The OA obtained with four different window lengths are shown for Flevoland dataset in Fig. 3. 20 features are extracted in each method. For all methods (CLPP-MP, CLPP-GLCM and CLPP-Gabor), $L = 13$ achieves the highest OA among the tested lengths. Note that increasing the window length increases the computation time and memory requirement. From the other hand, larger neighborhood windows may include the dissimilar samples from different classes in the extended training set, which may degrade the classification accuracy.

B) Classification results

Efficiency of CLPP is assessed from the classification accuracy point of view by using the contextual cubes of MP, GLCM and Gabor. Three PCs of PolSAR datasets are used for doing these experiments. The window length of neighborhood region is set as $L = 7$, and 18 features are extracted in each method.

At first, the classification results without applying the guided filter is investigated. The classification results containing the class accuracies, average accuracy, OA and kappa coefficient are reported in Table I for Flevoland dataset. The associated values of Z scores obtained from the McNemars test are also represented in Table II. The ground truth map (GTM), Pauli RGB and classification maps are shown in Fig. 4. According to the obtained results, the use of CLPP approach generally improves the classification

[DOI: 10.52547/itrc.13.2.29]

accuracy with respect to conventional methods where the MP, GLCM and Gabor feature cubes are given to the SVM classifier with the original training samples and without applying the feature transformation. In addition, the highest accuracy is achieved by CLPP-MP. Another finding is better performance of Gabor compared to the GLCM.

The classification results for SanFrancisco dataset are represented in Tables III and IV and also Fig. 5. Similar to previous dataset, CLPP-MP ranks first. CLPP-MP is better than MP and CLPP-GLCM is better than GLCM. But, Gabor results in better classification results compared to CLPP-Gabor. The Z-scores of the McNemars test in Tables II and IV show that the difference between classification results of each pair of methods reported in Tables I and III are statistically significant or not. The behavior of the proposed algorithm is also assessed when the guided filter is used to smooth the classification results. The classification accuracies for Flevoland and SanFrancisco datasets are reported in Tables V and VI, respectively. According to the obtained results, the highest overall accuracy is obtained by CLPP-MP in both datasets. The use of CLPP improves the classification accuracy for GLCM in both datasets. But, the use of CLPP does not lead to classification improvement when Gabor filter bank is used for contextual feature extraction. The classification maps for two datasets are shown in Figs. 6-7. As seen, applying the guided filtering to the classification maps smooth them significantly. The McNemars test results reported in Table VII and VIII show significant difference of CLPP methods compared to conventional ones from the statistical point of view.

To have a comparison among the classification results when guided filter is used or not, the OA of two datasets are briefly represented in Table IX. It can be found that the use of guided filtering significantly improves the classification results in both datasets. In both cases of “with guided filtering” and “without guided filtering”, CLPP-MP works better than MP, CLPP-GLCM works better than GLCM but CLPP-Gabor works worse than Gabor. In other words, dimensionality reduction of Gabor features degrades the classification results.

The running time of different methods are reported in Table X. As seen, the use of CLPP approach increases the running time for three contextual feature cubes (MP, GLCM and Gabor). This finding is expected because CLPP does some revisions on the initial classification map obtained by the contextual feature cubes. According to the obtained results, among MP, GLCM and Gabor spatial feature extractors, MP is the fastest and GLCM is the slowest operator. Correspondingly, among CLPP-MP, CLPP-GLCM and CLPP-Gabor methods, the CLPP-MP has the lowest running time while CLPP-GCLM has the highest running time. As a general conclusion, CLPP-MP can be the best candid for PolSAR image classification because not only it provides the highest classification accuracy but also it implements faster than the other competitors.

IV. Conclusion

The CLPP method is proposed for PolSAR image classification using limited training samples. The CLPP method at first extracts the contextual features for providing an initial classification map. Then, it adds the neighbors with the same class labels to the training set. CLPP applies a supervised locality preserving projection on the polarimetric-contextual feature cubes to find the reduced feature cubes. The obtained features are used to provide a new classification map. Finally, the guided filter is optionally applied to the classification map to degrade the speckle noise and achieve a smoothed classification map. According to the experimental results, CLPP results in higher classification accuracy compared to the full channels contextual cubes. Among MP, GLCM and Gabor, generally MP ranks first and Gabor ranks second.

References

[1] P. Wang, W. Chen, S. Gou, X. Zhang, X. Li and L. Jiao, "A weighted joint sparse of three channels method for full POL-SAR data classification," *2017 IEEE International Geoscience and Remote Sensing Symposium (IGARSS)*, Fort Worth, TX, pp. 6146-6149, 2017.

[2] O. Frey and E. Meier, "3-D Time-Domain SAR Imaging of a Forest Using Airborne Multibaseline Data at L- and P-Bands," in *IEEE Transactions on Geoscience and Remote Sensing*, vol. 49, no. 10, pp. 3660-3664, Oct. 2011.

[3] M. Imani, "Texture Feed Based Convolutional Neural Network for Pansharpening," Neurocomputing, vol. 398, pp. 117–130, 2020.

[4] H. Liu, F. Shang, S. Yang, M. Gong, T. Zhu and L. Jiao, "Sparse Manifold-Regularized Neural Networks for Polarimetric SAR Terrain Classification," in *IEEE Transactions on Neural Networks and Learning Systems*, vol. 31, no. 8, pp. 3007-3016, Aug. 2020.

[5] W. Hua, W. Xie and X. Jin, "Three-Channel Convolutional Neural Network for Polarimetric SAR Images Classification," in *IEEE Journal of Selected Topics in Applied Earth Observations and Remote Sensing*, vol. 13, pp. 4895-4907, 2020.

[6] Q. Yin, J. Cheng, F. Zhang, Y. Zhou, L. Shao and W. Hong, "Interpretable POLSAR Image Classification Based on Adaptive-Dimension Feature Space Decision Tree," in *IEEE Access*, vol. 8, pp. 173826-173837, 2020.

[7] X. Nie, R. Gao, R. Wang and D. Xiang, "Online Multiview Deep Forest for Remote Sensing Image Classification via Data Fusion," in *IEEE Geoscience and Remote Sensing Letters, In Press*, 2021.

[8] Q. Wu, B. Hou, Z. Wen, Z. Ren and L. Jiao, "Cost-Sensitive Latent Space Learning for Imbalanced PolSAR Image

[DOI: 10.52547/itrc.13.2.29]

Classification," in *IEEE Transactions on Geoscience and Remote Sensing, In Press*, 2021.
[9] S. Luo, K. Sarabandi, L. Tong and L. Pierce, "A SAR Image Classification Algorithm Based on Multi-Feature Polarimetric Parameters Using FOA and LS-SVM," in *IEEE Access*, vol. 7, pp. 175259-175276, 2019.
[10] M. Imani, "3D Gabor Based Hyperspectral Anomaly Detection," AUT Journal of Modeling and Simulation, vol. 50, no. 2, pp. 189-194, 2018.
[11] O. Yuzugullu, E. Erten and I. Hajnsek, "Rice Growth Monitoring by Means of X-Band Co-polar SAR: Feature Clustering and BBCH Scale," in *IEEE Geoscience and Remote Sensing Letters*, vol. 12, no. 6, pp. 1218-1222, June 2015.
[12] M. Imani, "Anomaly detection using morphology-based collaborative representation in hyperspectral imagery," European Journal of Remote Sensing, vol. 51, no. 1, pp. 457–471, 2018.
[13] Zhaocong Wu and Qundong Ouyang, "SVM- and MRF-based method for contextual classification of polarimetric SAR images," *2011 International Conference on Remote Sensing, Environment and Transportation Engineering*, Nanjing, pp. 818-821, 2011.
[14] Z. Zhang, H. Wang, F. Xu and Y. Jin, "Complex-Valued Convolutional Neural Network and Its Application in Polarimetric SAR Image Classification," *IEEE Transactions on Geoscience and Remote Sensing*, vol. 55, no. 12, pp. 7177-7188, 2017.
[15] M. Imani and H. Ghassemian, "Morphology-based structure-preserving projection for spectral–spatial feature extraction and classification of hyperspectral data, IET Image Processing, vol. 13, no. 2, pp. 270-279, Feb. 2019.
[16] X. Kang, S. Li and J. A. Benediktsson, "Spectral–Spatial Hyperspectral Image Classification With Edge-Preserving Filtering," in *IEEE Transactions on Geoscience and Remote Sensing*, vol. 52, no. 5, pp. 2666-2677, May 2014.
[17] M. Imani, "A Random Patches Based Edge Preserving Network for Land Cover Classification Using Polarimetric Synthetic Aperture Radar Images," International Journal of Remote Sensing, 2021.
[18] F. Mirzapour and H. Ghassemian, "Using GLCM and Gabor filters for classification of PAN images," 21st Iranian Conference on Electrical Engineering (ICEE 2013), Mashhad, Iran, May 2013.
[19] M. Imani, H. Ghassemian, "GLCM, Gabor, and Morphology Profiles Fusion for Hyperspectral Image Classification," 24th Iranian Conference on Electrical Engineering, Shiraz, Iran, pp. 460-465,10-12 May 2016.

Maryam Imani completed her Ph.D in Electrical Engineering, Communication, from Tarbiat Modares University, Tehran, Iran in 2015. She continued her research in Tarbiat Modares University as a postdoc. From 2018 to now, she is an Assistant professor of the Faculty of Electrical and Computer Engineering at Tarbiat Modares University, Tehran, Iran. Her research interests include Remote Sensing, Statistical Pattern Recognition, Signal and Image Processing, Information Analysis, and Machine Learning.

[DOI: 10.52547/itrc.13.2.29]